

Deep Learning based Multi-Source Localization with Source Splitting and its Effectiveness in Multi-Talker Speech Recognition

Aswin Shanmugam Subramanian^{a,*}, Chao Weng^c, Shinji Watanabe^{b,a}, Meng Yu^d, Dong Yu^d

^aCenter for Language and Speech Processing, Johns Hopkins University, Baltimore, MD, USA

^bLanguage Technologies Institute, Carnegie Mellon University, Pittsburgh, PA, USA

^cTencent AI Lab, Shenzhen, China

^dTencent AI Lab, Bellevue, WA, USA

Abstract

Multi-source localization is an important and challenging technique for multi-talker conversation analysis. This paper proposes a novel supervised learning method using deep neural networks to estimate the direction of arrival (DOA) of all the speakers simultaneously from the audio mixture. At the heart of the proposal is a source splitting mechanism that creates source-specific intermediate representations inside the network. This allows our model to give source-specific posteriors as the output unlike the traditional multi-label classification approach. Existing deep learning methods perform a frame level prediction, whereas our approach performs an utterance level prediction by incorporating temporal selection and averaging inside the network to avoid post-processing. We also experiment with various loss functions and show that a variant of earth mover distance (EMD) is very effective in classifying DOA at a very high resolution by modeling inter-class relationships. In addition to using the prediction error as a metric for evaluating our localization model, we also establish its potency as a frontend with automatic speech recognition (ASR) as the downstream task. We convert the estimated DOAs into a feature suitable for ASR and pass it as an additional input feature to a strong multi-channel and multi-talker speech recognition baseline. This added input feature drastically improves the ASR performance and gives a word error rate (WER) of 6.3% on the evaluation data of our simulated noisy two speaker mixtures, while the baseline which doesn't use explicit localization input has a WER of 11.5%. We also perform ASR evaluation on real recordings with the overlapped set of the MC-WSJ-AV corpus in addition to simulated mixtures.

Keywords: source localization, multi-talker speech recognition

1. Introduction

Source localization, also known as direction of arrival (DOA) estimation, is the task of estimating the direction of the sound sources with respect to the microphone array. This localization knowledge can aid many downstream applications. For example, they are used in robot audition systems [1, 2] to facilitate interaction with humans. Source localization is pivotal in making the human-robot communication more natural by rotating the robot's head. The localization component in the robot audition pipeline also aids in source separation and recognition. Moreover, there is growing interest in using far-field systems to process multi-talker conversations like meeting transcription [3]. Incorporating the source localization functionality can enrich such systems by monitoring the location of speakers and also potentially help improve the performance of the downstream automatic speech recognition (ASR) task. DOA estimation can also be used with smart speaker scenarios [4, 5] and potentially aid with better audio-visual fusion.

*Corresponding Author. A part of the work was carried out by this author during an internship at Tencent AI Lab, Bellevue, USA.

Email addresses: aswin@jhu.edu (Aswin Shanmugam Subramanian), cweng@tencent.com (Chao Weng), shinjiw@ieee.org (Shinji Watanabe), raymondmyu@tencent.com (Meng Yu), dyu@tencent.com (Dong Yu)

Some of the earlier DOA estimation techniques are based on narrowband subspace methods [6, 7]. The simple wideband approximation can be achieved by using the incoherent signal subspace method (ISSM), which uses techniques such as multiple signal classification (MUSIC) independently on narrowband signals of different frequencies and average their results to obtain the final DOA estimate. Broadband methods which better utilize the correlation between different frequencies such as weighted average of signal subspaces (WAVES) [8] and test of orthogonality of projected subspaces (TOPS) [9] have shown promising improvements. Alternative cross-correlation based methods like steered response power with phase transform (SRP-PHAT) [10] have also been proposed. All these previously mentioned methods are based on signal processing, and they are not robust to reverberations as they were developed under a free-field propagation model [11]. Recently, there has been a shift in interest to supervised deep learning methods to make the estimation robust to challenging acoustic conditions .

The initial deep learning methods were developed for single source scenarios [12, 13, 14, 15, 16]. In [12] and [13], features are extracted from MUSIC and GCC-PHAT respectively. The learning is made more robust in [14, 15, 16] by encapsulating the feature extraction inside the neural network. While [13] treats DOA estimation as a regression problem, all the other methods formulate it as a classification problem by discretizing the possible DOA angles. The *modeling resolution* which is determined by the output dimension of the network is quite low in [12], [14], and [16] at 5° , 45° , and 5° respectively. Although the modeling resolution is high in [15] with classes separated by just 1° , the evaluation was performed only with a block size of 5° and it is also shown to be not robust to noise.

The deep learning models were extended to handle multiple source cases by treating it as a multi-label classification problem in [17, 11, 18]. This still gives only a single vector as output with each dimension treated as a separate classification problem. This procedure is not good at capturing the intricate inter-class relationship in our problem. So increasing the number of classes to perform classification at a very high resolution will fail. During inference, the output vector is treated like a spatial spectrum and DOAs are estimated based on its peaks. In [18, 17], the number of peaks is determined based on a threshold. In [11], the number of sources are assumed to be known based on which the peaks are chosen at the output. In [17] and [11], the source locations are restricted to be only in a spatial grid with a step size of 10° and 15° respectively. To make the models work on realistic conditions, it is crucial to handle all possible source locations. Moreover, these models perform a frame level prediction in spite of the sources assumed to be stationary inside an utterance. Hence, post-processing is required to get the utterance level DOA estimate.

In this work, we propose a *source splitting* mechanism, which involves treating the neural network as two distinct and well defined components. The first component disentangles the input mixture by implicitly splitting them as source-specific hidden representations. The second component then maps these features to as many DOA posteriors as the number of sources in the mixture. This makes the number of classification problems to be only equal to the number of sources and not the the number of DOA classes like the existing methods. With the added help of loss functions that can handle the inter-class relationship better, our methods can classify DOA reliably at a high resolution. Like [11], we assume the knowledge of number of sources in the utterance but we incorporate it directly in the architecture of the model instead of using it while post-processing.

We evaluate our proposed localization method both as a standalone task and also based on its effectiveness as a frontend to aid speech recognition. Assuming the DOA to be known, the effectiveness of using features extracted from the ground-truth location for target speech recognition was shown in [19, 20] as a proof of concept. The importance of localization for multi-talker speech recognition was also shown in our previous work [21]. In [21], we proposed a model named *directional ASR* (D-ASR), which can learn to predict DOA without explicit supervision by joint optimization with speech recognition. D-ASR replaces the typical separation subnetwork used in multi-talker speech recognition with a localization subnetwork. Although D-ASR works well for clean speech mixtures, it is not robust to additive stationary noise. In the second part of this paper, we devise a more robust approach to D-ASR that can improve multi-talker speech recognition. We use a strong multi-talker speech recognition system called MIMO-Speech [22, 23] as a baseline. The DOAs estimated from our proposed models in the first part are converted to angle features [19]. These features are given as additional inputs to the MIMO-Speech model and tested for its effectiveness in improving speech recognition. It is hard to obtain DOA labels for real datasets. We perform DOA estimation for real speech

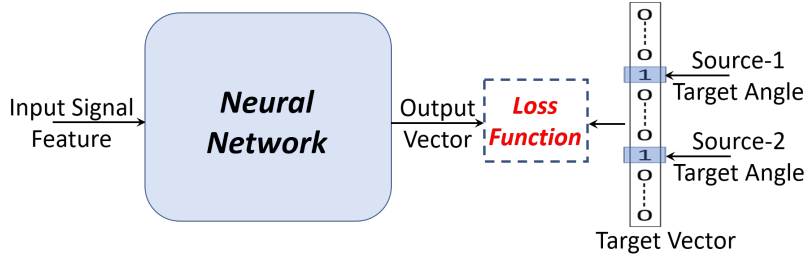


Figure 1: Multi-label Classification Model for 2-source Scenario

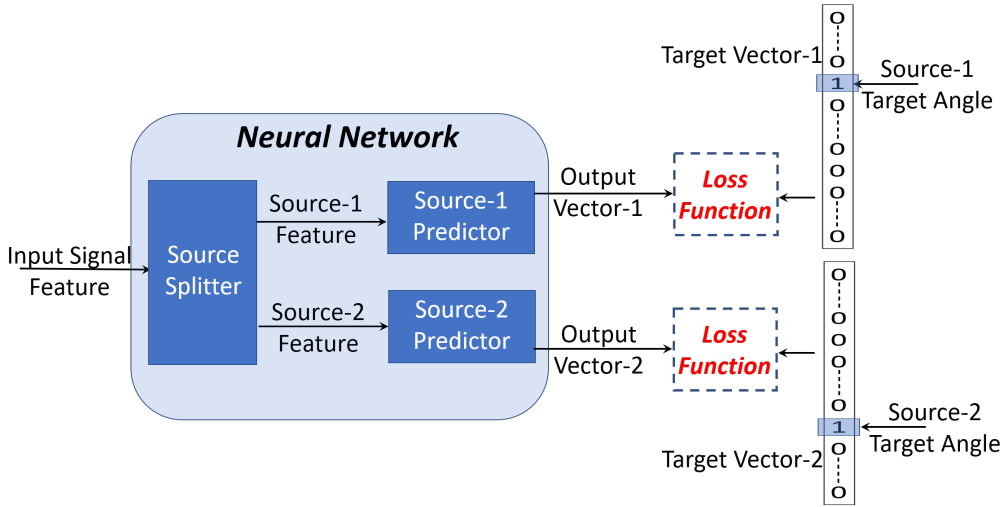


Figure 2: Proposed Model with Source Splitting Mechanism for 2-source Scenario

mixtures from multichannel wall street journal audio-visual (MC-WSJ-AV) corpus and evaluate the quality of localization solely based on the downstream ASR metric of word error rate (WER).

2. Deep Learning based Multi-Source Localization

Given a multi-channel input signal with multiple sources, a deep neural network can be trained to predict all the azimuth angles corresponding to each of the sources. Typically it is treated as a multi-label classification problem [11, 17], as shown in Figure 1. Here, the network outputs only a single vector which is supposed to encode the DOA of all the sources. It is possible to have spurious peaks in angle classes that are in close proximity to any of the target angle classes, especially when the number of classes are increased. As more than one peak needs to be selected from the vector during inference, it is possible a spurious peak will also be chosen at the expense of a different source.

We propose an alternative modeling approach for multi-source localization. In this model, the network is divided into two well-defined components with specific functionalities as shown in Figure 2. The first component is the *source splitter*, which dissects the input mixed signal to extract source specific spatial features. These features are passed to the second component named *source dependent predictors*, which gives individual posterior vectors as output. As multiple outputs are obtained, each one has a well defined target with just one target angle corresponding to a specific source.

As we will have N output predictions corresponding to the N sources in our proposed model, there will be source permutation ambiguity in how we assign the predictions to the targets. We handle it in two ways. First we can use permutation invariant training (PIT) [24] that are popular for source separation models.

In PIT, all possible prediction-target assignment permutations are considered a valid solution and the one with the minimum loss is chosen during training. Alternatively, we fix the target angles to be in ascending order and force only this permutation.

Although the sources are stationary in existing models like [11], a frame level prediction is performed and then time averaging is used as a post processing step during inference. It is common in tasks like speaker identification, which involve converting a sequence of features into a vector to incorporate average pooling inside the network [25, 26]. We follow this approach in all our models to avoid post-processing.

We describe the different deep learning architectures used in this work. First we describe an architecture based on multi-label classification. Then we introduce two different architectures based on our proposed source splitting mechanism. Let Y_1, Y_2, \dots, Y_M be the M -channel input signal in the short-time Fourier transform (STFT) domain, with $Y_m \in \mathbb{C}^{T \times F}$, where T is the number of frames and F is the number of frequency components. The input signal is reverberated, consisting of N speech sources. There can be additive stationary noise but we assume that there are no point source noises. We also assume that N is known. In this work the array geometry is considered to be a uniform circular arrays (UCA) and only the azimuth angle is estimated.

2.1. CNN-BLSTM Model with Multi-label Classification (CNN-BLSTM-MLC)

This model is designed to take the raw multi-channel phase as the feature. Let the phase spectrum of the multichannel input signal be represented as $\mathcal{P} \in [0, 2\pi]^{T \times M \times F}$. This raw phase \mathcal{P} is passed through the first component of the localization network based on a convolutional neural network (CNN) given by LocNet-CNN(\cdot) to extract phase feature Z by pooling the channels as follows:

$$Z = \text{LocNet-CNN}(\mathcal{P}) \in \mathbb{R}^{T \times Q}, \quad (1)$$

where Q is the feature dimension. The LocNet-CNN(\cdot) architecture is inspired from [11], which uses convolutional filters across the microphone-channel dimension to learn phase difference like features.

The phase feature Z from Eq. (1) is passed through a bidirectional long short-term memory (BLSTM) component LocNet-BLSTM-MLC(\cdot) as follows,

$$W = \text{LocNet-BLSTM-MLC}(Z), \quad (2)$$

where $W \in \mathbb{R}^{T \times Q}$ is an intermediate feature. We consider that the sources are stationary within an utterance. So in the next step a simple time average is performed to obtain a summary vector.

$$\xi(q) = \frac{1}{T} \sum_{t=1}^T w(t, q), \quad (3)$$

where $\xi(q)$ is the summary vector at dimension q , and $w(t, q)$ is the intermediate feature at time t and feature dimension q . The summary vector, represented in vector form as $\boldsymbol{\xi} \in \mathbb{R}^Q$ is passed through a learnable AffineLayer(\cdot) to convert its dimension to $\lfloor 360/\gamma \rfloor$, where γ is the angle resolution in degrees to discretize the DOA angle.

$$\boldsymbol{\kappa} = \sigma(\text{AffineLayer}(\boldsymbol{\xi})). \quad (4)$$

$$(5)$$

where, $\sigma(\cdot)$ is the sigmoid activation, and $\boldsymbol{\kappa} \in (0, 1)^{\lfloor 360/\gamma \rfloor}$ is the multi-label classification vector. The DOAs can be estimated by finding the indices in $\boldsymbol{\kappa}$ corresponding to the N largest peaks.

2.2. CNN-BLSTM Model with Source Splitting Mechanism (CNN-BLSTM-SS)

This architecture is inspired from the localization subnetwork used in D-ASR [21]. This model also uses raw phase as the input and the phase feature Z is extracted in the same way as Section 2.1 using Eq. (1). Z will have DOA information about all the sources in the input signal. It is processed by the next component LocNet-Mask(\cdot) which consists of BLSTM layers. Source splitting is achieved through this component which extracts source-specific binary masks as follows,

$$[W^n]_{n=1}^N = \sigma(\text{LocNet-Mask}(Z)), \quad (6)$$

where $W^n \in [0, 1]^{T \times Q}$ is the feature mask for source n and $\sigma(\cdot)$ is the sigmoid activation. This mask segments Z into regions that correspond to each source. Note that LocNet-Mask(\cdot) can also implicitly perform voiced activity detection as it outputs binary masks.

The extracted phase mask from Eq. (6) is used to perform a weighted averaging of the phase feature from Eq. (1) to get source-specific summary vectors. The summary vector will encode the DOA information specific to a source as the masks are used as weights to summarize information only from the corresponding source regions in the following way,

$$\xi^n(q) = \frac{\sum_{t=1}^T w^n(t, q) z(t, q)}{\sum_{t=1}^T w^n(t, q)}, \quad (7)$$

where $\xi^n(q)$ is the summary vector for source n at dimension q , $w^n(t, q) \in [0, 1]$ and $z(t, q) \in \mathbb{R}$ are the extracted feature mask (for source n) and the phase feature, respectively, at time t and feature dimension q .

The summary vector, represented in vector form as $\xi^n \in \mathbb{R}^Q$ is passed through a learnable source-specific AffineLayer $^n(\cdot)$, which acts as the predictor and converts the summary vector from dimension Q to the dimension $\lfloor 360/\gamma \rfloor$, where γ is the angle resolution in degrees to discretize the DOA angle. Based on this discretization, we can predict the DOA angle as a classifier with the softmax operation. From this, we can get the source-specific posterior probability for the possible angle classes as follows,

$$[\Pr(\theta^n = \alpha_i | \mathcal{P})]_{i=1}^{\lfloor 360/\gamma \rfloor} = \text{Softmax}(\text{AffineLayer}^n(\xi^n)), \quad (8)$$

$$\alpha_i = ((\gamma * i) - ((\gamma - 1)/2)) (\pi/180), \quad (9)$$

The estimated DOA $\hat{\theta}^n$ for source n is determined by finding the peak from the corresponding posterior in Eq. (8) as follows,

$$\hat{\theta}^n = \underset{\alpha_i}{\text{argmax}} \Pr(\theta^n = \alpha_i | \mathcal{P}), \quad (10)$$

2.3. BLSTM Model with Source Splitting Mechanism (BLSTM-SS)

In this model, inter-microphone phase difference (IPD) is computed and passed as a feature directly to the model. There are no CNN layers in this model as pre-defined features are used. The binary masking is also removed in this model to estimate the summary vectors in a more direct way. The IPD features are calculated as,

$$\bar{p}_i(t, f) = \frac{1}{M} [\cos \angle(\frac{y_{i_1}(t, f)}{y_{i_2}(t, f)}) + j \sin \angle(\frac{y_{i_1}(t, f)}{y_{i_2}(t, f)})], i = 1 : I, \quad (11)$$

where $y_m(t, f)$ is the input signal at channel m , time t and frequency f , i represents an entry in a microphone pair list defined for calculating the IPD; and i_1 and i_2 are the index of microphones in each pair. We calculate IPD features for I pairs and then concatenate their real and imaginary parts together. The concatenated

IPD feature is represented as $\bar{\mathcal{P}} \in \mathbb{R}^{T \times I \times 2F}$. The magnitude of the input signal at channel 1 i.e. $|Y_1|$ is also added as a feature to give the final input feature $\bar{\mathcal{Z}} \in \mathbb{R}^{T \times (2IF+F)}$. This feature is passed to a BLSTM component LocNet-BLSTM(\cdot), which is the source splitter, as follows,

$$[\bar{W}^n]_{n=1}^N = \sigma(\text{LocNet-BLSTM}(\bar{\mathcal{Z}})), \quad (12)$$

where $\bar{W}^n \in \mathbb{R}^{T \times Q}$ is the source-specific feature for source n . As we don't have a binary mask in this model, we take a simple average instead of the weighted average used in Eq. (7) to extract the summary vector as follows,

$$\bar{\xi}^n(q) = \frac{1}{T} \sum_{t=1}^T \bar{w}^n(t, q), \quad (13)$$

The summary vector is used similar to Section 2.2 and the source specific DOAs are obtained by following Eq. (8) and Eq. (10).

2.4. Loss Functions

The multi-label classification model in Section 2.1 is trained with the binary cross entropy (BCE) loss. The models in Section 2.2 and Section 2.3 give source-specific probability distributions at the output. So cross entropy (CE) loss will be the natural choice. This choice will be good for a typical classification problem where the inter-class relationship is not important. As we are estimating the azimuth angles, we have classes that are ordered. So it is better to optimize by taking the class relationships into account as they are very informative.

Typically a 1-hot vector is given as target to the CE loss. In DOA estimation it is better to predict a nearby angle compared to a far away angle. But the typical penalty from the CE loss doesn't take this into account. A loss function that takes the class ordering into account is the earth mover distance (EMD). EMD is the minimal cost required to transform one distribution to another [27]. As in our problem the classes are naturally in a sorted order, we can use the simple closed-form solution from [28]. The solution is given by the squared error between the cumulative distribution function(CDF) of the prediction and the target probability distributions.

Another way to induce inter-class relationship is by using a soft target probability distribution which is not as sparse as the 1-hot vector. We use the following target distribution:

$$\chi(i) = \begin{cases} 0.4 & i = \psi \\ 0.2 & i = (\psi \pm 1) \% [360/\gamma] \\ 0.1 & i = (\psi \pm 2) \% [360/\gamma] \\ 0 & elsewhere \end{cases} \quad (14)$$

where, $\chi(i)$ is the probability weight of the target distribution for class i and ψ is the index corresponding to the target angle class. When this soft target distribution is used with CE, we define it as the *soft cross entropy* (SCE) loss. Similarly, it can also be used with EMD and we define it as *soft earth mover distance* (SEMD) loss. By assigning some probability weight to the angle classes in the neighbourhood of the target, the network can be potentially made to learn some inter-class relationship.

3. Integration of Localization with ASR

MIMO-Speech [22, 23] is an end-to-end neural network that can perform simultaneous multi-talker speech recognition by taking the mixed speech multi-channel signal as the input. The MIMO-Speech network consists of three main components: (1) The masking subnetwork, (2) differentiable minimum variance

distortionless response (MVDR) beamformer, and (3) the ASR subnetwork. The masking network in MIMO-Speech is monaural and gives channel-dependent time-frequency masks for beamforming. For this only the magnitude of the corresponding channel is given as input to the masking network. We will modify this masking network to take composite multi-channel input and output a channel-independent mask which will be shared across all channels.

Firstly, it is possible to also get a multi-channel masking network baseline by using \bar{Z} from Section 2.3 as the composite feature which is the concatenation of IPD features from Eq. (11) and the magnitude of the first channel. For this to be further extended to take localization knowledge we need to concatenate it with an additional input feature that can encode the estimated azimuth angle. The groundtruth DOA is encoded as angle features in [19, 20, 29]. We follow the same procedure but use the estimated DOA from our models proposed in Section 2.

The steering vector $\mathbf{d}^n(f) \in \mathbb{C}^M$ for source n and frequency f is calculated from estimated DOA $\hat{\theta}^n$. In this work we have used uniform circular arrays (UCA) and the steering vector is calculated as follows,

$$\tau_m^n = \frac{r}{c} \cos(\hat{\theta}^n - \psi_m), \quad m = 1 : M \quad (15)$$

$$\mathbf{d}^n(f) = [e^{j2\pi f \tau_1^n}, e^{j2\pi f \tau_2^n}, \dots, e^{j2\pi f \tau_M^n}], \quad (16)$$

where τ_m^n is the signed time delay between the m -th microphone and the center for source n , ψ_i is the angular location of microphone m , r is the radius of the UCA and c is the speed of sound (343 m/s).

The calculated steering vector is used to compute the angle features with the following steps,

$$\tilde{a}^n(t, f) = |\mathbf{d}^n(f)^H \mathbf{y}(t, f)|^2, \quad (17)$$

$$\mathbf{a}^n(t, f) = \tilde{a}^n(t, f) * \mathcal{I}(\tilde{a}^n(t, f) - \tilde{a}^s(t, f))_{s=1:N}, \quad (18)$$

where $\mathbf{a}^n(t, f)$ is the angle feature for source n at time t and frequency f , H is conjugate transpose, $\mathbf{y}(t, f) \in \mathbb{C}^M$ is the multichannel input, N is the number of speakers, and $\mathcal{I}(\cdot)$ is the indicator function that outputs 0 if the input difference is negative for any of the “ $s = 1 : N$ ” cases and 1 otherwise.

The computed angle features for all the sources are concatenated and included to the composite feature input list that is fed to the multi-channel masking network. This subnetwork given by MaskNet(\cdot) gives the source specific masks $L^n \in (0, 1)^{T \times F}$ as the output. Rest of the procedure is similar to the original MIMO-Speech model. The masks are used to compute the source specific spatial covariance matrix (SCM), $\Phi^n(f)$ as follows:

$$\Phi^n(f) = \frac{1}{\sum_{t=1}^T l^n(t, f)} \sum_{t=1}^T l^n(t, f) \mathbf{y}(t, f) \mathbf{y}(t, f)^H, \quad (19)$$

The interference SCM, $\Phi_{\text{intf}}^n(f)$ for source n is approximated as $\sum_{i \neq n}^N \Phi^i(f)$ like [22] (we experiment only with $N = 2$, so no summation in that case). From the computed SCMs, the M -dimensional complex MVDR beamforming filter [30] for source n and frequency f , $\mathbf{b}_{\text{MVDR}}^n(f) \in \mathbb{C}^M$ is estimated as,

$$\mathbf{b}_{\text{MVDR}}^n(f) = \frac{[\Phi_{\text{intf}}^n(f) + \Phi_{\text{noise}}(f)]^{-1} \Phi^n(f)}{\text{Tr}([\Phi_{\text{intf}}^n(f) + \Phi_{\text{noise}}(f)]^{-1} \Phi^n(f))} \mathbf{u}, \quad (20)$$

where $\mathbf{u} \in \{0, 1\}^M$ is a one-hot vector to choose a reference microphone, $\text{Tr}(\cdot)$ denotes the trace operation, and $\Phi_{\text{noise}}(f)$ is the noise SCM. The noise SCM can be estimated by obtaining an additional mask from the masking network. However we consider only stationary noise in this study and we experimentally found that it was better to ignore the noise SCM by considering it as an all-zero matrix.

With the estimated MVDR filter, we can perform speech separation to obtain the n -th separated STFT signal, $x^n(t, f) \in \mathbb{C}$ as follows:

$$x^n(t, f) = \mathbf{b}^n(f)^H \mathbf{y}(t, f), \quad (21)$$

This separated signal for source n , represented in matrix form as $X^n \in \mathbb{C}^{T \times F}$ is transformed to a feature suitable for speech recognition by performing log Mel filterbank transformation and utterance based mean-variance normalization (MVN). The extracted feature O^n for source n is passed to the speech recognition subnetwork $\text{ASR}(\cdot)$ to get $C^n = (c_1^n, c_2^n, \dots)$, the token sequence corresponding to source n . The MIMO-Speech network is optimized with the reference text transcriptions $[C_{ref}^i]_{i=1}^N$ as the target. The joint connectionist temporal classification (CTC)/attention loss [31] is used as the ASR optimization criteria.

Here again there is permutation ambiguity as there are multiple output sequences. We can solve it in two ways. First, we can follow the PIT scheme similar to the original MIMO-Speech model to resolve the prediction-target token sequence assignment problem. This takes additional computation time. We propose to use the DOA knowledge to resolve the ambiguity in the following way. During training stage, we can use the groundtruth DOA as input instead of the estimated DOA for computing the angle features. We determine the permutation of the target sequence based on the order of sources in which the angle features are concatenated and thereby can eliminate PIT.

4. Experiments

4.1. Data & Setup

Table 1: The configurations used for simulating the clean & noisy 2-speaker mixtures

	<i>Clean 2-mix</i>	<i>Noisy 2-mix</i>
Simulation corpus	WSJ0	WSJCAM0
ASR pretraining corpus	WSJ	WSJ
Noise corpus	N/A	REVERB challenge
Sampling rate	16 KHz	16 KHz
Num. utterances	Train - 12776 Dev - 1206 Eval - 651	Train - 7860 Dev - 742 Eval - 1088
num. RIR	Train- 3194 Dev - 1206 Eval - 651	Train - 2620 Dev - 742 Eval - 1088
T60	0.15 - 0.5 s	0.25 - 0.7 s
Num. channels	6	8
UCA radius	5cm	10cm
Source distance from array	1.5 - 3m	1 - 2m
SNR	N/A	10 - 20 dB

We simulated two types of 2-speaker mixtures: (1) clean mixtures that don't have any additive stationary noise simulated from the subset WSJ0 of the wall street journal (WSJ) corpus [32], which is same as used in [21], (2) noisy mixtures from WSJCAM0 [33] that also uses noise from REVERB corpus [34]. The noisy mixtures are generated with the same array geometry as REVERB and also the real MC-WSJ-AV [35] corpus. The 5k vocabulary subset of the real overlapped data with stationary sources from MC-WSJ-AV

was used just for evaluation with the models trained with the noisy mixtures. For each utterance, we mixed another utterance from a different speaker within the same set, so the resulting simulated data is the same size as the original clean data. The SMS-WSJ [36] toolkit was used for creating the simulated data with maximum overlap. Image method [37] was used to create the room impulse responses (RIR). Room configurations with the size (length-width-height) ranging from 5m-5m-2.6m to 11m-11m-3.4m were used while creating both types of mixtures. Both sources and the array are always chosen to be at the same height. The other configuration details used for simulation are shown in Table 1

For the six microphone array the following pair list: (1, 4), (2, 5), (3, 6), (1, 2), (3,4), and (5, 6) were used to compute the IPD features defined in Eq (11). The pair list for the eight microphone array was: (1, 5), (2, 6), (3, 7), (4, 8), (1, 3), (3,5), (5,7), and (7, 1). Three CNN blocks with rectified linear unit (ReLU) activation after each block followed by a feedforward layer were used as LocNet-CNN(\cdot) defined in Eq. (1). The CNN filters are applied across the channel-frequency dimensions. The kernel shapes were dependent on the number of input channels. For 6-microphone configuration kernels of shapes, 3×1 , 2×3 , and 3×3 were used for the first, second, and third CNN block respectively. The shapes were 4×1 , 3×3 , and 3×3 for 8-microphone case. Padding was not performed for the channel dimension so as to fuse them after the final CNN block. The number of feature maps were 4 in the first block, 16 in the second block, and 32 in the final block. Q was fixed as " $2 \times \lfloor 360/\gamma \rfloor$ ". One output gate projected bidirectional long short-term memory (BLSTMP) layer with Q cells was used as LocNet-Mask(\cdot) defined in Eq. (6).

The masking network for MIMO-Speech was designed with two BLSTMP layers with 771 cells. The encoder-decoder ASR network was based on the Transformer architecture [38] and it was initialized with a pretrained model that used single speaker training utterances from both WSJ0 and WSJ1. The same architecture as [23] was used for the encoder-decoder ASR model. It has 12 layers in the encoder and 6 layers in the decoder. Before the Transformer encoder, the log Mel filterbank features of 80 dimensions are encoded by two CNN blocks. The CNN layers have a kernel size of 3×3 and the number of feature maps is 64 in the first block and 128 in the second block. Attention/CTC joint ASR decoding was performed with score combination with a word-level recurrent language model from [39] trained on the text data from WSJ. Our implementation was based on the Pytorch backend of ESPnet [40].

The input signal was preprocessed with weighted prediction error (WPE) [41, 42] based dereverberation with a filter order of 10 and prediction delay 3, only during inference time. The second channel was fixed as the reference microphone for MVDR in Eq. (20). We evaluate several localization models with the proposed DOA integration with MIMO-Speech. To avoid retraining every time, the groundtruth DOA was used while training the network and DOA estimation was performed only while inference. While PIT training, the order of the angle features was randomly permuted. Subspace DOA estimation was performed with "Pyroomacoustics" toolkit [43].

4.2. Multi-Source Localization Performance

We use two popular subspace-based signal processing methods MUSIC and TOPS as baselines. For both, the spatial response is computed and the top two peaks are detected to estimate the DOA. The results of D-ASR is also shown for comparison. The average absolute cyclic angle difference between the predicted angle and the ground-truth angle in degrees is used as the metric. The permutation of the prediction with the reference that gives the minimum error is chosen.

The results with and without WPE preprocessing for both the clean and noisy mixtures are given in Table 2. Most of the supervised deep learning models with different configurations perform significantly better than the subspace methods. We can see that MUSIC and TOPS are not very sensitive to the difference in angle resolution (γ). The results show that the deep learning methods are robust to reverberations and give good results even without the WPE frontend. D-ASR [21] results from row 5 perform very well on the clean mixture but we can see that it is not robust to noise. The results of D-ASR on the noisy mixture is much worse compared to even the subspace methods.

The results of the multi-label classification model from Section 2.1 are given in rows 6 & 7, We can see that a higher resolution of $\gamma = 5$ degrades the performance from $\gamma = 10$. This is because of spurious peaks in nearby angles when the resolution is increased. This shows the need for having separate output vectors for

Table 2: DOA absolute prediction error on both our clean and noisy simulated 2-source mixtures comparing our proposed source-splitting methods with subspace methods, multi-label classification, & D-ASR

Row ID	Method	γ	Loss Function	PIT	Clean Mixture				Noisy Mixture			
					No Dev	WPE Test	WPE Dev	WPE Test	No Dev	WPE Test	WPE Dev	WPE Test
1	MUSIC	1	-	-	22.5	24.0	15.6	14.4	19.5	17.3	12.3	11.1
2	MUSIC	10	-	-	23.2	21.7	13.5	12.6	21.3	18.8	17.4	15.0
3	TOPS	1	-	-	20.0	18.7	11.7	10.1	13.3	9.7	15.0	13.2
4	TOPS	10	-	-	20.4	19.4	13.3	10.6	14.1	10.3	16.7	14.9
5	D-ASR	10	ASR	✓	3.0	3.0	2.5	2.5	35.0	34.3	36.6	34.0
6	CNN-BLSTM-MLC	5	BCE	✗	26.3	28.4	25.4	25.0	19.9	21.6	20.8	20.7
7	CNN-BLSTM-MLC	10	BCE	✗	15.1	14.2	15.7	15.4	7.8	8.4	9.1	9.0
8	CNN-BLSTM-SS	10	CE	✓	4.4	4.4	4.1	4.1	6.4	7.5	6.7	6.9
9	CNN-BLSTM-SS	10	CE	✗	3.3	3.5	3.2	3.3	4.0	4.7	3.3	3.4
10	CNN-BLSTM-SS	1	CE	✓	23.9	24.1	26.3	23.9	34.7	35.7	34.3	37.0
11	CNN-BLSTM-SS	1	CE	✗	9.3	10.2	9.7	11.4	32.9	34.1	28.9	27.4
12	CNN-BLSTM-SS	1	SCE	✓	3.8	4.1	3.9	4.3	12.1	13.6	12.0	12.6
13	CNN-BLSTM-SS	1	SCE	✗	4.6	4.2	4.2	5.1	3.7	3.6	3.6	3.8
14	CNN-BLSTM-SS	1	EMD	✓	4.8	4.9	4.8	4.8	3.4	3.9	3.4	3.8
15	CNN-BLSTM-SS	1	EMD	✗	2.2	1.9	2.0	1.8	3.2	3.3	3.6	3.6
16	CNN-BLSTM-SS	1	SEMD	✓	1.6	1.4	1.4	1.5	2.8	2.6	2.8	2.9
17	CNN-BLSTM-SS	1	SEMD	✗	1.6	1.7	1.6	1.5	1.5	1.4	1.1	1.1
18	BLSTM-SS	1	SEMD	✓	1.5	1.6	1.5	1.7	2.3	2.2	2.2	2.5
19	BLSTM-SS	1	SEMD	✗	1.3	1.4	1.3	1.3	2.1	2.0	2.3	2.1

different sources. Rows 8-19 gives the results of the models with the proposed source splitting mechanism. The results on all configurations are given with both PIT and also fixing the targets in ascending order. From the results we can see that fixing the target order works better.

Rows 8-17 use the CNN-BLSTM-SS model proposed in Section 2.2 with phase feature masking. The CE loss with $\gamma = 10$ (rows 8, 9) works reasonably well and gives an improvement over the multi-label classification model. Increasing the resolution to $\gamma = 1$ (rows 10, 11) makes it poor because of its inability to learn inter-class relationship like explained in Section 2.4. Making the target distribution smoother with SCE loss alleviates the problem quite well and we can observe better results from row 13. Using EMD loss makes it very robust and works well also while using PIT training (row 14). Combining both ideas with the SEMD loss gives the best performance with a prediction error of around 1.5° when PIT is not used (row 17). The results of BLSTM-SS model (row 19) are a bit worse on the noisy mixture compared to the CNN-BLSTM-SS model.

4.3. ASR Performance

The speech recognition performance of our proposed DOA integration compared with the vanilla MIMO-Speech baseline is given in Table 3. Word error rate (WER) is used as the metric for ASR and the results are shown for both clean and noisy mixtures. The results of the clean single-speaker data with the pretrained ASR model is given in row 1. Note that the results of the clean single-speaker data used for the noisy mixture is not very good because it is from the British English corpus WSJCAM and the pretrained model was trained with American English data from WSJ. This accent difference is fixed in the mixed speech models as the ASR network will be fine tuned in that case with British English data. The ASR results of the simulated mixture using the single-speaker model is also shown (WER more than 100% because of too many insertion errors).

Oracle experiment by directly giving the reference ideal binary masks (IBM) to the beamformer is given in row 3. We can see that D-ASR works quite well on the clean mixture like shown in [21] but it is not

Table 3: ASR performance on the simulated clean & noisy 2-speaker mixtures comparing our proposed DOA integration method with vanilla MIMO-Speech. Word error rate (WER) is used as the metric for comparison. For WER, lower the better.

	Row ID	DOA Method	DOA PIT	IPD for ASR	ASR PIT	Clean Mixture Dev	Clean Mixture Test	Noisy Mixture Dev	Noisy Mixture Test
Clean	1	-	-	✗	✗	2.1	1.6	13.7	13.6
Input mixture (ch-1)	2	-	-	✗	✗	105.0	107.1	112.1	116.3
Oracle binary Mask (IBM)	3	-	-	✗	✗	3.6	3.0	7.1	6.5
D-ASR	4	CNN-BLSTM	-	✗	✓	5.1	4.1	23.3	21.5
Baseline MIMO-Speech	5	-	-	✗	✓	6.6	5.1	15.1	13.6
	6	-	-	✓	✓	5.8	4.4	13.1	11.5
MIMO-Speech + Oracle Angle Feature	7	-	-	✓	✓	3.5	2.7	6.8	6.0
	8	-	-	✓	✗	3.5	2.9	6.6	6.2
MIMO-Speech + DOA Estimation	9	MUSIC	-	✓	✓	15.1	14.8	13.3	12.5
	10	TOPS	-	✓	✓	21.0	20.7	14.9	13.6
	11	CNN-BLSTM-SS	✗	✓	✓	3.7	2.9	7.0	6.3
	12	CNN-BLSTM-SS	✗	✓	✗	3.7	2.9	7.0	6.3
	13	BLSTM-SS	✓	✓	✓	3.8	3.2	7.3	6.8
	14	BLSTM-SS	✗	✓	✓	3.6	2.9	7.3	6.7
	15	BLSTM-SS	✗	✓	✗	3.6	3.1	7.2	6.9

robust to noise. Row 5 shows the results of the baseline MIMO-Speech with the architecture originally proposed in [23]. Row 6 shows the modified baseline by adding IPD features and a channel independent masking network as mentioned in Section 3. This makes the baseline stronger and gives slightly better results. Oracle ASR-DOA integration experiments were performed by using the groundtruth DOA while inference as a proof of concept and the results are shown in rows 7 & 8. We can see a very significant improvement in this case and for the noisy mixture the word error rates are reduced by a factor of two. The results are also slightly better than using the oracle binary masks. This proves the importance of feeding localization knowledge to a multi-speaker ASR system. We can also see that turning off PIT and fixing the target sequence order based on the DOA order gives similar performance (row 8) with added benefits. This not only saves computation time while training but also makes the inference more informative by associating the DOA and its corresponding transcription.

In rows 9-15 some of the DOA estimation methods are used to compute the angle features. All the methods here are high resolution and use $\gamma = 1$. We can see that using MUSIC and TOPS degrades the ASR performance from the baseline. This shows that localization knowledge will be useful only if we can estimate with good precision and reliability. The results with the proposed deep learning based DOA estimation and SEMD loss are shown in rows 11-15. With any of these methods we get results close to using the oracle DOA. We can see the CNN-BLSTM-SS model which gives the best localization performance in Table 2 also gives the best results here (row 12). This result almost matches the performance obtained with oracle masks in row 3.

4.4. Real Data & Array Selection

In this section the overlapped data from MC-WSJ-AV corpus [35] is used for evaluation. The positions of the speakers are mentioned to be stationary throughout the utterance. There are six possible positions in the room that the speakers were positioned. As there are two speakers in the mixture, there are fifteen possible position pairs. The real data has recordings from two arrays with the same configuration placed in different positions. From the schematic diagram given in [35], four of the six positions are very close to array-1 and all positions are generally far from Array-2. The model trained with the simulated noisy mixture is used here as they follow similar configurations. Although trained with simulated data, it is crucial to see how our methods work on real data. As there are no groundtruth DOA labels, we cannot evaluate the angle prediction error.

The DOA estimation here is performed with $\gamma = 1$ and the CNN-BLSTM-SS model here is without PIT and with SEMD loss. As we know that there are fifteen position pairs, we performed k-means clustering

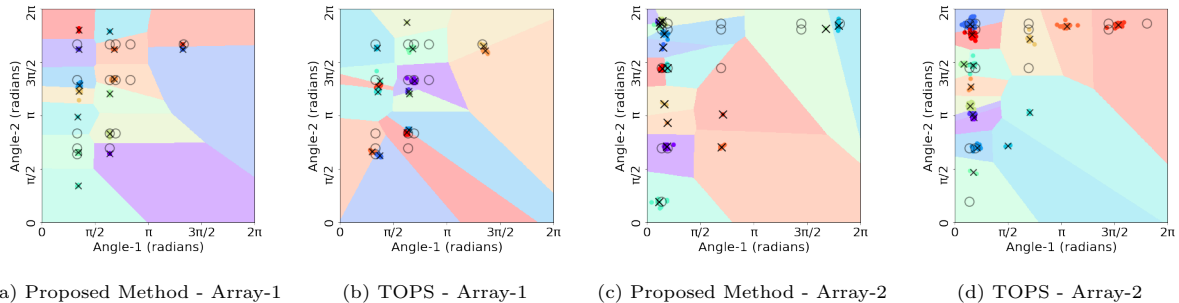


Figure 3: Results of k-means clustering with the estimated azimuth angle pairs of the real 2-speaker overlapped data from MC-WSJ-AV. The approximate groundtruth location are marked as black circles and the estimated cluster centers are given by black cross marks.

Table 4: ASR performance on the real 2-speaker overlapped data from MC-WSJ-AV. Word error rate (WER) is used as the metric for comparison. For WER, lower the better.

	<i>DOA Method</i>	<i>Array-1</i>	<i>Array-2</i>	<i>Combination</i>
MIMO-Speech	N/A	34.3	47.6	N/A
MIMO-Speech w/ IPD	N/A	29.6	44.9	N/A
MIMO-Speech + DOA Integration	MUSIC	11.4	31.0	25.2
MIMO-Speech + DOA Integration	TOPS	10.9	32.9	27.1
MIMO-Speech + DOA Integration	CNN-BLSTM-SS	14.0	18.2	11.7

with $k = 15$ on the estimated DOA pairs of all utterances. The pairs were ordered in an ascending order such that the lower angle comes first. The visualization of the clusters (cross marks are cluster centers) for both arrays obtained with the proposed method and TOPS are shown in Figure 3. From the schematic diagram of the recording setup given in [35] we calculated approximate source positions and they are also marked as black circles. There seems to be a reasonable level of agreement between the estimated positions from localization and the approximate groundtruths.

The ASR performance is shown in Table 4. Using estimated DOAs from either the subspace method or the CNN-BLSTM-SS model, ASR-DOA integration significantly outperforms the MIMO-Speech baselines for this data. This further proves the importance of localization as a very pivotal frontend for ASR. From the results we can see the positions of the sources are chosen to be favorable to array-1 so it gives better results. Using the subspace methods outperforms the CNN-BLSTM-SS model for array-1. Whereas for the challenging array-2 data, the proposed CNN-BLSTM-SS model significantly outperforms the subspace methods.

We perform a combination with an array selection scheme. The scheme is based on the intuition that it is not good to use an array when the sources have a very small angle difference from its perspective. Array-1 is given preference during the selection but if the angle difference between the sources is less than 10° , array-2 data is selected. We can see the selection mechanism to be effective with CNN-BLSTM-SS model but still it is slightly worse than the Array-1 results of the subspace methods. The selection mechanism doesn't help with subspace methods as its array-2 estimation is quite bad.

5. Conclusion & Future Work

We proposed a novel deep learning based model for multi-source localization that can classify DOAs with a high resolution. An extensive evaluation was performed with different choices of architectures, loss functions, classification resolution, and training schemes that handle permutation ambiguity. Our source splitting model was shown to have a significantly lower prediction error compared to both multi-label

classification model and subspace methods. We also proposed a soft earth mover distance (SEMD) loss function for the localization task that models inter-class relationship well for DOA estimation and hence predicts near perfect DOA.

We have also devised a method to use the proposed DOA estimation as a frontend for multi-talker ASR. This integration greatly helps speech recognition and shows the importance of using localization priors with far-field ASR models. Based on this finding, ASR performance was used as the metric of evaluation for DOA estimation in real data where DOA labels are not available to compute prediction errors.

In future, we would like to extend our methods to also handle source counting within the model to make it work for arbitrary number of sources. One possible approach would be to use a conditional chain model that is popular for source separation [44, 45]. The other important extension is adapting our method to work on more challenging and realistic data like CHiME-6 [46] which involves a complicated distributed array setup with moving sources.

References

- [1] K. Nakadai, T. Takahashi, H. Okuno, H. Nakajima, Y. Hasegawa, H. Tsujino, Design and implementation of robot audition system ‘HARK’ - open source software for listening to three simultaneous speakers, *Advanced Robotics* 24 (5-6) (2010) 739–761.
- [2] K. Nakadai, K. Hidai, H. Mizoguchi, H. Okuno, H. Kitano, Real-time auditory and visual multiple-object tracking for humanoids, in: *International Joint Conferences on Artificial Intelligence (IJCAI)*, 2001, pp. 1425–1432.
- [3] T. Yoshioka, I. Abramovski, C. Aksoylar, Z. Chen, M. David, D. Dimitriadis, Y. Gong, I. Gurvich, X. Huang, Y. Huang, A. Hurvitz, L. Jiang, S. Koubi, E. Krupka, I. Leichter, C. Liu, P. Parthasarathy, A. Vinnikov, L. Wu, X. Xiao, W. Xiong, H. Wang, Z. Wang, J. Zhang, Y. Zhao, T. Zhou, Advances in online audio-visual meeting transcription, in: *IEEE Automatic Speech Recognition and Understanding Workshop (ASRU)*, 2019, pp. 276–283.
- [4] J. Barker, S. Watanabe, E. Vincent, J. Trmal, The fifth CHiME speech separation and recognition challenge: Dataset, task and baselines, in: *Interspeech*, 2018, pp. 1561–1565.
- [5] R. Haeb-Umbach, S. Watanabe, T. Nakatani, M. Bacchiani, B. Hoffmeister, M. L. Seltzer, H. Zen, M. Souden, Speech processing for digital home assistants: Combining signal processing with deep-learning techniques, *IEEE Signal processing magazine* 36 (6) (2019) 111–124.
- [6] R. Schmidt, Multiple emitter location and signal parameter estimation, *IEEE transactions on antennas and propagation* 34 (3) (1986) 276–280.
- [7] R. Roy, T. Kailath, ESPRIT-estimation of signal parameters via rotational invariance techniques, *IEEE Transactions on Acoustics, Speech, and Signal Processing* 37 (7) (1989) 984–995.
- [8] E. D. Di Claudio, R. Parisi, WAVES: weighted average of signal subspaces for robust wideband direction finding, *IEEE Transactions on Signal Processing* 49 (10) (2001) 2179–2191.
- [9] Yeo-Sun Yoon, L. M. Kaplan, J. H. McClellan, TOPS: new doa estimator for wideband signals, *IEEE Transactions on Signal Processing* 54 (6) (2006) 1977–1989.
- [10] J. DiBiase, A high-accuracy, low-latency technique for talker localization in reverberant environments using microphone arrays, PhD Thesis, Brown University.
- [11] S. Chakrabarty, E. A. Habets, Multi-speaker DOA estimation using deep convolutional networks trained with noise signals, *IEEE Journal of Selected Topics in Signal Processing* 13 (1) (2019) 8–21.
- [12] R. Takeda, K. Komatani, Sound source localization based on deep neural networks with directional activate function exploiting phase information, in: *IEEE International Conference on Acoustics, Speech, and Signal Processing (ICASSP)*, 2016, pp. 405–409.
- [13] F. Vesperini, P. Vecchiotti, E. Principi, S. Squartini, F. Piazza, A neural network based algorithm for speaker localization in a multi-room environment, in: *26th IEEE International Workshop on Machine Learning for Signal Processing (MLSP)*, 2016, pp. 1–6.
- [14] T. Hirvonen, Classification of spatial audio location and content using convolutional neural networks, in: *138th Audio Engineering Society Convention*, Vol. 2, 2015.
- [15] N. Yalta, K. Nakadai, T. Ogata, Sound source localization using deep learning models, *Journal of Robotics and Mechatronics* 29 (2017) 37–48.
- [16] S. Chakrabarty, E. A. Habets, Broadband doa estimation using convolutional neural networks trained with noise signals, in: *IEEE Workshop on Applications of Signal Processing to Audio and Acoustics (WASPAA)*, 2017, pp. 136–140.
- [17] S. Adavanne, A. Politis, T. Virtanen, Direction of arrival estimation for multiple sound sources using convolutional recurrent neural network, in: *European Signal Processing Conference (EUSIPCO)*, 2018, pp. 1462–1466.
- [18] W. He, P. Motlicek, J. Odobez, Deep neural networks for multiple speaker detection and localization, in: *IEEE International Conference on Robotics and Automation (ICRA)*, 2018, pp. 74–79.
- [19] Z. Chen, X. Xiao, T. Yoshioka, H. Erdogan, J. Li, Y. Gong, Multi-channel overlapped speech recognition with location guided speech extraction network, in: *IEEE Spoken Language Technology Workshop (SLT)*, 2018, pp. 558–565.
- [20] A. S. Subramanian, C. Weng, M. Yu, S. Zhang, Y. Xu, S. Watanabe, D. Yu, Far-field location guided target speech extraction using end-to-end speech recognition objectives, in: *IEEE International Conference on Acoustics, Speech, and Signal Processing (ICASSP)*, 2020, pp. 7299–7303.

- [21] A. S. Subramanian, C. Weng, S. Watanabe, M. Yu, Y. Xu, S.-X. Zhang, D. Yu, Directional ASR: A new paradigm for e2e multi-speaker speech recognition with source localization (2020). [arXiv:2011.00091](https://arxiv.org/abs/2011.00091).
- [22] X. Chang, W. Zhang, Y. Qian, J. Le Roux, S. Watanabe, MIMO-Speech: End-to-end multi-channel multi-speaker speech recognition, in: IEEE Automatic Speech Recognition and Understanding Workshop (ASRU), 2019, pp. 237–244.
- [23] X. Chang, W. Zhang, Y. Qian, J. Le Roux, S. Watanabe, End-to-end multi-speaker speech recognition with transformer, in: IEEE International Conference on Acoustics, Speech, and Signal Processing (ICASSP), 2020, pp. 6134–6138.
- [24] D. Yu, M. Kolbæk, Z. Tan, J. Jensen, Permutation invariant training of deep models for speaker-independent multi-talker speech separation, in: IEEE International Conference on Acoustics, Speech, and Signal Processing (ICASSP), 2017, pp. 241–245.
- [25] D. Snyder, D. Garcia-Romero, G. Sell, D. Povey, S. Khudanpur, X-Vectors: Robust dnn embeddings for speaker recognition, in: IEEE International Conference on Acoustics, Speech, and Signal Processing (ICASSP), 2018, pp. 5329–5333.
- [26] K. Veselý, S. Watanabe, K. Žmolíková, M. Karafiát, L. Burget, J. H. Černocký, Sequence summarizing neural network for speaker adaptation, in: IEEE International Conference on Acoustics, Speech, and Signal Processing (ICASSP), 2016, pp. 5315–5319.
- [27] E. Levina, P. Bickel, The earth mover’s distance is the mallows distance: some insights from statistics, in: IEEE International Conference on Computer Vision (ICCV), Vol. 2, 2001, pp. 251–256.
- [28] L. Hou, C.-P. Yu, D. Samaras, Squared earth mover’s distance-based loss for training deep neural networks, NeurIPS Workshop - Learning on Distributions, Functions, Graphs and Groups.
- [29] F. Bahmaninezhad, J. Wu, R. Gu, S.-X. Zhang, Y. Xu, M. Yu, D. Yu, A Comprehensive Study of Speech Separation: Spectrogram vs Waveform Separation, in: Interspeech, 2019, pp. 4574–4578.
- [30] M. Souden, J. Benesty, S. Affes, On optimal frequency-domain multichannel linear filtering for noise reduction, IEEE Transactions on Audio, Speech, and Language Processing 18 (2) (2010) 260–276.
- [31] S. Kim, T. Hori, S. Watanabe, Joint CTC-attention based end-to-end speech recognition using multi-task learning, in: ICASSP, 2017, pp. 4835–4839.
- [32] D. B. Paul, J. M. Baker, The design for the wall street journal-based CSR corpus, in: Proceedings of the workshop on Speech and Natural Language, Association for Computational Linguistics, 1992, pp. 357–362.
- [33] T. Robinson, J. Franssen, D. Pye, J. Foote, S. Renals, WSJCAMO: a British English speech corpus for large vocabulary continuous speech recognition, in: IEEE International Conference on Acoustics, Speech, and Signal Processing (ICASSP), Vol. 1, 1995, pp. 81–84.
- [34] K. Kinoshita, M. Delcroix, S. Gannot, E. A. Habets, R. Haeb-Umbach, W. Kellermann, V. Leutnant, R. Maas, T. Nakatani, B. Raj, et al., A summary of the REVERB challenge: state-of-the-art and remaining challenges in reverberant speech processing research, EURASIP Journal on Advances in Signal Processing.
- [35] M. Lincoln, I. McCowan, J. Vepa, H. K. Maganti, The multi-channel wall street journal audio visual corpus (mc-wsj-av): specification and initial experiments, in: IEEE Workshop on Automatic Speech Recognition and Understanding, 2005, pp. 357–362.
- [36] L. Drude, J. Heitkaemper, C. Boeddeker, R. Haeb-Umbach, SMS-WSJ: Database, performance measures, and baseline recipe for multi-channel source separation and recognition, arXiv preprint arXiv:1910.13934.
- [37] J. B. Allen, D. A. Berkley, Image method for efficiently simulating small-room acoustics, The Journal of the Acoustical Society of America 65 (4) (1979) 943–950.
- [38] S. Karita, N. Chen, T. Hayashi, T. Hori, H. Inaguma, Z. Jiang, M. Someki, N. E. Y. Soplin, R. Yamamoto, X. Wang, S. Watanabe, T. Yoshimura, W. Zhang, A comparative study on Transformer vs RNN in speech applications, in: IEEE Automatic Speech Recognition and Understanding Workshop (ASRU), 2019, pp. 449–456.
- [39] T. Hori, J. Cho, S. Watanabe, End-to-end speech recognition with word-based RNN language models, in: IEEE Spoken Language Technology Workshop (SLT), 2018, pp. 389–396.
- [40] S. Watanabe, T. Hori, S. Karita, T. Hayashi, J. Nishitoba, Y. Unno, N. Enrique Yalta Soplin, J. Heymann, M. Wiesner, N. Chen, A. Renduchintala, T. Ochiai, ESPnet: End-to-end speech processing toolkit, in: Interspeech, 2018, pp. 2207–2211.
- [41] T. Nakatani, T. Yoshioka, K. Kinoshita, M. Miyoshi, B. Juang, Speech dereverberation based on variance-normalized delayed linear prediction, IEEE Transactions on Audio, Speech, and Language Processing 18 (7) (2010) 1717–1731.
- [42] L. Drude, J. Heymann, C. Boeddeker, R. Haeb-Umbach, NARA-WPE: A Python package for weighted prediction error dereverberation in Numpy and Tensorflow for online and offline processing, in: ITG Fachtagung Sprachkommunikation, 2018.
- [43] R. Scheibler, E. Bezzam, I. Dokmanić, Pyroomacoustics: A python package for audio room simulation and array processing algorithms, in: IEEE International Conference on Acoustics, Speech, and Signal Processing (ICASSP), 2018, pp. 351–355.
- [44] K. Kinoshita, L. Drude, M. Delcroix, T. Nakatani, Listening to each speaker one by one with recurrent selective hearing networks, in: IEEE International Conference on Acoustics, Speech, and Signal Processing (ICASSP), 2018, pp. 5064–5068.
- [45] J. Shi, X. Chang, P. Guo, S. Watanabe, Y. Fujita, J. Xu, B. Xu, L. Xie, Sequence to multi-sequence learning via conditional chain mapping for mixture signals, Advances in Neural Information Processing Systems.
- [46] S. Watanabe, M. Mandel, J. Barker, E. Vincent, A. Arora, X. Chang, S. Khudanpur, V. Manohar, D. Povey, D. Raj, D. Snyder, A. S. Subramanian, J. Trmal, B. B. Yair, C. Boeddeker, Z. Ni, Y. Fujita, S. Horiguchi, N. Kanda, T. Yoshioka, N. Ryant, CHiME-6 challenge:tackling multispeaker speech recognition for unsegmented recordings (2020). [arXiv:2004.09249](https://arxiv.org/abs/2004.09249).